Hindawi Publishing Corporation
Journal of Nanotechnology
Volume 2011, Article ID 702130, 6 pages
doi:10.1155/2011/702130

Research Article

Enhancement in Photoelectrochemical Efficiency by Fabrication of $BiVO_4$@MWCNT Nanocomposites

Yan Zhang,[1] Jianqiang Yu,[1] Hongwei Wang,[1] Mengmeng Sun,[2] Yuyu Bu,[3] Deshuang Yu,[1] and Weibing Li[3]

[1] *Key Laboratory of New Fiber Materials and Modern Textile, School of Chemistry, Chemical Engineering and Environments, Qingdao University, 308 Ningxia Road, Qingdao 266071, China*
[2] *Institute of Oceanology, Chinese Academy of Science, Qingdao 266071, China*
[3] *Faculty of Environment and Safety, Qingdao University of Science and Technology, Qingdao 266042, China*

Correspondence should be addressed to Jianqiang Yu, jianqyu@qdu.edu.cn

Received 30 July 2011; Accepted 17 September 2011

Academic Editor: Yuanhui Zheng

An enormous enhancement in the photo-to-current conversion efficiency over the nanocomposite material composed by $BiVO_4$ on the surface of MWCNTs, with respect to electrode of pure $BiVO_4$, was observed. The heterojunction formed between MWCNTs and nano-$BiVO_4$ is beneficial for the separation of photogenerated electrons and holes, resulting in more electrons that are able to transport efficiently to the surface and therefore enhance the photoefficiency.

1. Introduction

Since the photoelectrochemical water splitting (the Honda-Fujishima effect) was reported in 1972 [1], great progresses have been made on the research and application of photocatalysis and photoelectrochemistry both in energy and environmental fields.

Up to date, the design and development of visible-light-responsive photocatalysts is one of the research directions, because the utilization of visible light, which accounts for more than half of the solar spectrum, is significant. For this goal, it is utmost important to develop photocatalysts with a narrow band gap. One of the efforts consists of creating an electron donor level between the valence band and conduction band of TiO_2 by doping with metallic or nonmetallic elements such as such as Ag, Cu, Fe, Co, V, Cr, and Pd and rare earth element or N, S, and C [2–10]. However, although the doping of foreign elements extends the absorption to visible-light ranges, it increases the defects of semiconductor photocatalysts, which therefore is a part of the ultraviolet light-responsive performance that the titanium oxide originally possessed was occasionally ruined [11–17]. Another effort is the exploring of complex compounds that containing Bi^{3+}, In^{3+}, Sn^{2+} (s^2 configuration), or Ag^+ (d^{10} configuration) ions in an oxide system. Thus, it is able to elevate the valence band by means of the hybridization of their respective orbitals with the O_{2p} orbital, and also narrowing the band gap of the semiconductor [18].

$BiVO_4$ is one of such complex oxides with narrow band gap. $BiVO_4$ shows not only excellent visible-light photocatalytic properties, but also a high photo-to-current conversion efficiency [19–27]. Almost a decade ago, the high activity of $BiVO_4$ for photocatalytic O_2 evolution from aqueous suspensions containing Ag^+ as a sacrificial electron acceptor under visible-light irradiation was observed [19]. It was then discovered that nanocrystalline $BiVO_4$ thin-film electrodes show high photocurrent yields for oxygen evolution in neutral aqueous electrolytes [25–27]. Therefore, $BiVO_4$ might be a good visible-light photovoltaic material. However, at the present stage, it is still necessary to explore strategies to improve the visible-light photoelectrochemical reactivity and efficiency of $BiVO_4$.

The photoelectrochemical properties can be enhanced if the photogenerated electrons or holes are transmitted effectively, in which the recombination of electrons and holes is avoided. As we have known, the rate of electron-hole

recombination is a decisive factor for photoelectrochemical properties. Thus, to form a heterojunction with semiconductor called a Schottky barrier, where there is a space-charge separation region, is an effective method of increasing recombination times for electron-hole pairs. Traditionally, this method of extending recombination times was established with platinum and other noble metal interfaces. CNTs have a variety of electronic properties, similar to the metals above mentioned, and they may also exhibit metallic conductivity as one of the many possible electronic structures [28]. The physical and chemical characteristics of semiconductor photocatalysts as well as the high conductivity along the tube axis of carbon nanotubes (CNTs) produced a great deal of incentive to disperse CNTs into the photoactive layer in order to obtain more efficient photoelectrochemical devices [29, 30]. However, the fabrication of nanosized $BiVO_4$ on the surface of MWCNTs to form a nanocomposite of $BiVO_4$@MWCNT was not reported in the literatures.

In this work, the photoelectrochemical property of the $BiVO_4$@MWCNT thin-film photoelectrode was studied, and an enhancement in the photo-to-current conversion efficiency was observed. The heterojunction formed between BiVO4 and CNTs as well as the direct electron transportation effect of carbon nanotube is proposed to charge for the enhancement of photoefficiency.

2. Experimental Section

2.1. Fabrication of $BiVO_4$@MWCNTs Nanocomposites. $BiVO_4$-MWCNTs nanocomposite was prepared by co-precipitation method. First, required amounts of $Bi(NO_3)_3 \cdot 5H_2O$ and NH_4VO_3 were separately dissolved in 2.0 mol/L of nitric acid solution. The pretreated MWCNTs (provided by Chengdu Organic Chemical Co. Ltd.) were dispersed into PEG in ultrasonic for 1 h. Then, the mixture of MWCNTs and PEG were added into the solution of $Bi(NO_3)_3$ and NH_4VO_3. Meantime, 5 g of urea was added into the above mixture. The solution was stirred at 353–363 K for 12 h. At last, the mixture was filtered, washed, and dried, and the $BiVO_4$@MWCNTs nanocomposite was received. For comparison, pure $BiVO_4$ was also prepared according to the procedure reported in the literature [23]. The electrodes were prepared using the above-synthesized powders by dip-coating on the ITO conductive glass.

2.2. The Photoelectrochemical Measurements. The photoelectrochemical properties were carried by CHI760C electrochemical work station (Shanghai Chenhua instrument Co., Ltd.) in a three-electrode cell setup with a flat circular quartz window (diameter = 2 cm) opposite the working electrode, and platinum wire and Ag/AgCl were used as counter and reference electrodes, respectively. The light source was a 300-W Xe arc lamp (PLS-SXE300, Beijing Changtuo Co. Ltd.), and the electrodes were illuminated from the back electrode of the ITO side with a 420 nm bandpass filter in front of a quartz window to remove the light of wavelength less than 420 nm. The electrolyte was 0.5 mol/L Na_2SO_4 solution without pH control.

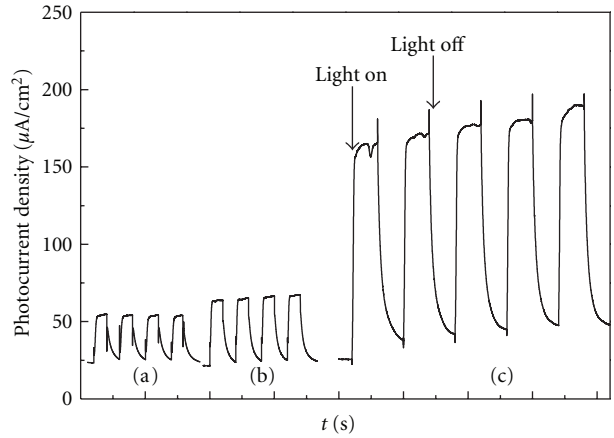

Figure 1: Photocurrent density over (a) pure $BiVO_4$, (b) mixture of $BiVO_4$ and MWCNTs, and (c) $BiVO_4$@MWCNTs composite films under visible light ($\lambda \geq 420$ nm).

3. Results and Discussions

3.1. The Enhanced Photoefficiency of $BiVO_4$@MWCNTs Nanocomposites. Figure 1 shows the photoelectrochemical behaviors of the thin-film photoelectrodes fabricated by pure $BiVO_4$, a mixture of $BiVO_4$ and MWCNTs, and $BiVO_4$@MWCNTs nanocomposite, which were measured by transient photocurrent-time curves. As can be seen from the current-time (I-t) curves, pure $BiVO_4$ thin-film electrode showed an intensive photocurrent density of about 30 μA/cm^2 under visible light ($\lambda \geq 420$ nm) irradiation. The photocurrent over the photoelectrode prepared from a mixture of $BiVO_4$ and CNT is increased in a certain extent with comparison to that over pure $BiVO_4$ photoelectrode, getting to 42 μA/cm^2. While it is interesting that the photocurrent intensity on $BiVO_4$@MWCNTs nanocomposite electrode is much higher than that over the above two electrodes, reaching to over 140 μA/cm^2. It should be noted that the amount of photoactive $BiVO_4$ in $BiVO_4$@MWCNTs nanocomposite and mixture of $BiVO_4$-MWCNTs is much lower than that of pure $BiVO_4$. So, it is unambiguously that the photocurrent over $BiVO_4$@MWCNTs nanocomposite photoelectrode was enhanced greatly with comparison to the pure $BiVO_4$ as well as $BiVO_4$-MWCNTs electrodes. As all of the semiconductors were prepared by coprecipitation method, while the only difference is just whether or not formation of nanocomposites of $BiVO_4$ with the MWCNTs, the enhanced photocurrents over photoelectrodes of $BiVO_4$@MWCNTs suggested that the formation of nanocomposite structure of $BiVO_4$@MWCNTs is the major factor for improving the photo-to-current conversion efficiency.

3.2. The Structure of $BiVO_4$@MWCNTs Nanocomposites. The crystalline structure of $BiVO_4$ and the morphologies of the formatted composites with carbon nanotube were characterized by X-ray diffraction pattern and electron microscopy. Figure 2 shows the XRD patterns of pure $BiVO_4$, $BiVO_4$@MWCNTs nanocomposite, and MWCNTs, respectively. The diffraction peaks of pure $BiVO_4$ prepared

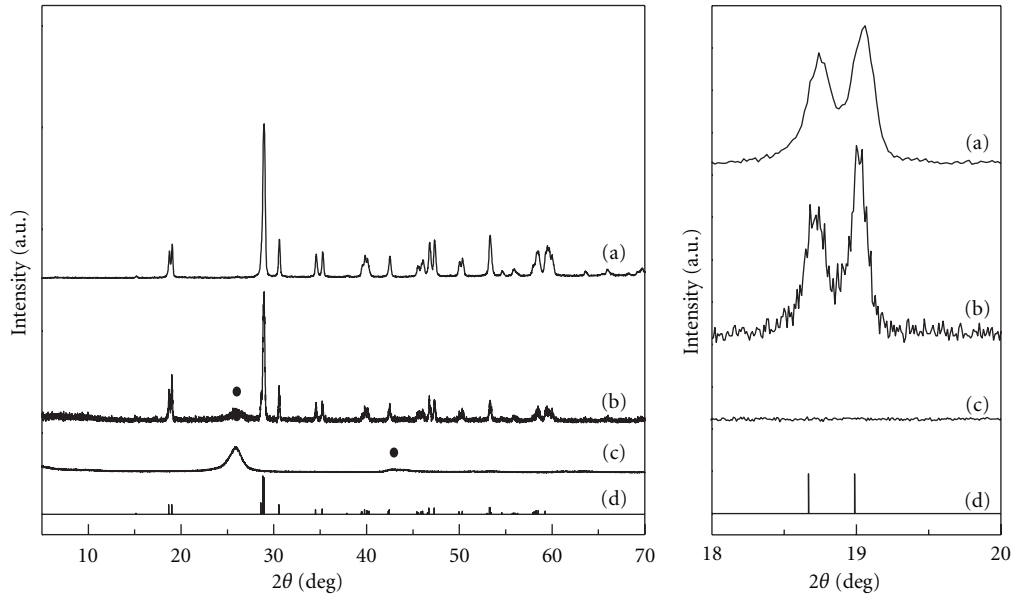

Figure 2: XRD patterns of (a) pure $BiVO_4$ nanoparticles, (b) $BiVO_4$@MWCNTs nanoparticles, (c) MWCNTs, and (d) JCPDS card no. 14-0688.

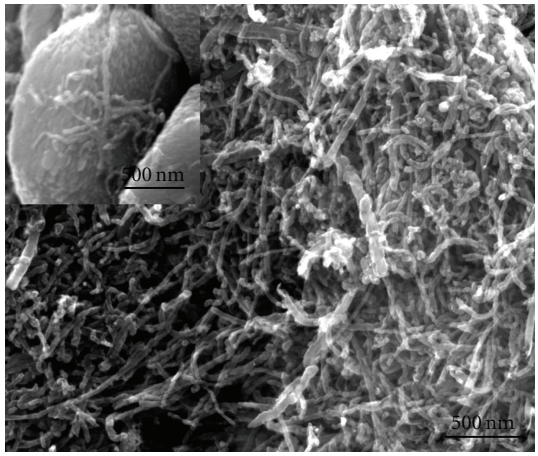

Figure 3: FE-SEM image of $BiVO_4$-MWCNTs. The insert shows the limited bulk $BiVO_4$ formed between MWCNTs.

by a coprecipitation process are in good agreement with the standard JCPDS card no. 14-0688. This structure is the typical monoclinic scheelite $BiVO_4$ (Figure 2(a)). No impurity peaks were observed, indicating that the sample is a pure phase $BiVO_4$ with a monoclinic scheelite structure. The XRD patterns of the $BiVO_4$@MWCNTs composites exhibit diffraction peaks much similar to the pure $BiVO_4$ powders except that two small peaks at 26.06° and 44.46° (indicated by dots in Figure 2), which are attributed to the characteristic peaks of MWCNTs (Figure 2(c)). These results suggested that the $BiVO_4$ particles in $BiVO_4$@MWCNTs composites sample are also of monoclinic scheelite phase.

In the three main crystal forms of $BiVO_4$ (tetragonal zircon type and monoclinic and tetragonal scheelite structure), monoclinic scheelite $BiVO_4$ is much more active than the tetragonal scheelite for O_2 evolution from aqueous $AgNO_3$ solution under visible-light irradiation [21]. The photo-to-current properties of monoclinic scheelite $BiVO_4$ was also found much intensive than the other two structures. This is because the tension in the microstructure of monoclinic scheelite $BiVO_4$ is more intensive than that of tetragonal scheelite, due to the presence of a $6s^2$ lone pair of Bi^{3+} resulted in the lone-pair distortion of the former one is much higher than the later one [21, 23]. These distinctive differences in the structure can be conveniently distinguished by XRD patterns, in which the monoclinic scheelite $BiVO_4$ with a high distortion generally shows well splitting of peaks at 18.5°, 35°, and 46° of 2θ. The widened part of XRD patterns near 19° of pure $BiVO_4$ and $BiVO_4$@MWCNTs composites are distinguished shown in the section of Figure 2(b). It can be observed that both samples showed two peaks with well resolution at this area. This observation suggested that both of the pure $BiVO_4$ and the $BiVO_4$@MWCNTs composites are of monoclinic scheelite type with a high distortion.

3.3. The Morphologies of $BiVO_4$@MWCNTs Nanocomposites. Figure 3 shows the typical morphologies of the $BiVO_4$@MWCNTs, which were examined by SEM. It is seen that most of $BiVO_4$ particles are nanosized that attached to the MWCNTs tightly. On the other hand, there are some bulks $BiVO_4$ particles that were observed among $BiVO_4$@MWCNTs nanoparticles, revealing that the particles free from the MWCNTs grow more readily than those on the MWCNTs (shown in the inset of Figure 3), and the diameter bulk particles reach to 1 μm. In the mean time, some of the MWCNTs attached tightly to the surface of the bulk $BiVO_4$.

Figure 4 shows the typical TEM photographs of pure MWCNTs and $BiVO_4$@MWCNTs. It is seen that $BiVO_4$ nanoparticles are attached on the wall of MWCNTs (Figure 4(b)), contrasting to the relative smooth surface of pure MWCNT (Figure 4(a)). The size of $BiVO_4$ nanoparticles

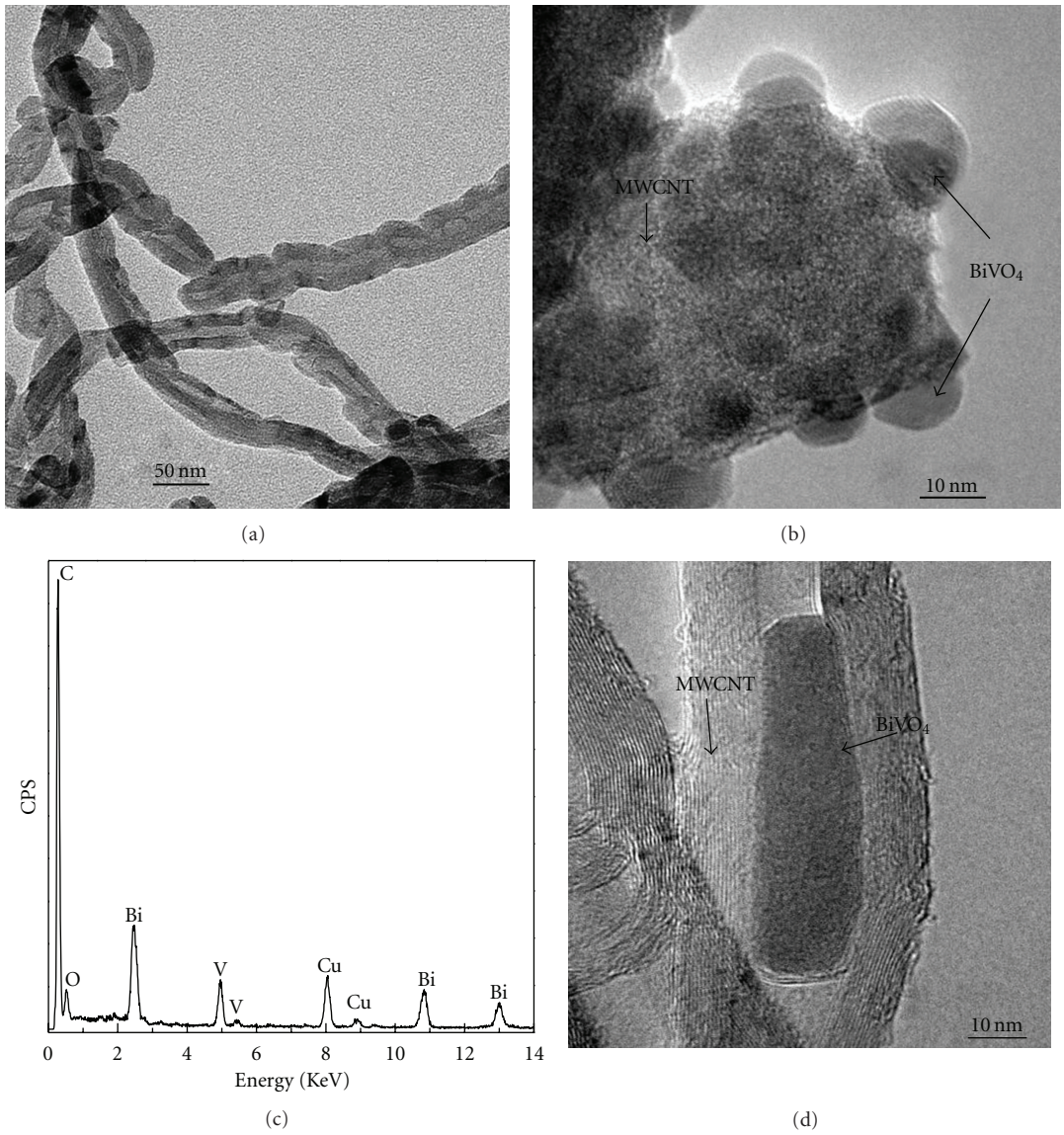

Figure 4: TEM images of (a) pure MWCNTs, (b, d) $BiVO_4$@MWCNTs, and (c) EDX spectrum of $BiVO_4$@MWCNTs.

is less than 10 nm, in the range of 5–10 nm. In addition, the $BiVO_4$ nanoparticles on the MWCNTs are significantly smaller than the particles of bulk $BiVO_4$, which should be attributed to the restriction effect of MWCNTs on the growth of attached nanoparticles. To investigate the composition of these tiny particles, EDX spectra analysis was applied to probe the composition of the coated nanoparticles (Figure 4(c)). It was found that V, Bi, O, C, and Cu elements are present on the surface of the nanotubes, revealing the existence of V and Bi on MWCNTs. The Cu signal arises from the copper grid and the C signal comes from the MWCNTs. Furthermore, the interface between MWCNT and $BiVO_4$ is clearly seen, indicating that $BiVO_4$ nanoparticles are well attached on the outermost shell of MWCNTs. Besides attaching on the surface of MWCNTs, $BiVO_4$ nanoparticles were also observed in the inner hollow cavity of nanotubes (shown in Figure 4(d)). It shows that nanosize cylinder in cavity of nanotubes is about 10 nm for the diameter and 40 nm for the length. However, the diameter of MWCNTs is just about 7-8 nm. The expansion force of the crystal growth of $BiVO_4$ led to the distortion of the nanotubes, while the suppression of the carbon wall resulted in the growth of crystal toward the tube axis, which is free of such hindrance.

3.4. The Structural Effect of Nanocomposites on the Photoefficiency. As we have observed, the photo-to-current efficiency of $BiVO_4$@MWCNTs nanocomposites has been enhanced enormously. The enhancement should be related to the structure of $BiVO_4$@MWCNTs nanocomposites. For a semiconductor thin-film electrode, the photocurrent should be controlled by the recombination probability of photogenerate electrons and holes. The higher rate of e^--h^+ recombination will lead to a low photocurrent, and thus a lower photoefficiency. Because the MWCNTs had a high electron

affinity and excellent conductivity, the exited electrons from photoactive $BiVO_4$ were trapped easily by MWCNTs and transferred quickly along CNT to the ITO conductive glass substrate. Consequently, an intensive current was observed. Moreover, the observations in the TEM micrographs of $BiVO_4$@MWCNTs suggested that the $BiVO_4$ nanoparticles are tightly attached with the surface of MWCNTs, and this tight attachment can form a heterojunction between the photoactive materials with CNT and lead to less boundaries exist between the two phases; therefore, less electrons losses occurred in the boundary. The heterojunction formed in the device can achieve charge separation and collection due to the tightly attachment of $BiVO_4$ with MWCNTs. Due to the introduction of internal junctions of $BiVO_4$/nanotube within the nanocomposite matrix, the high electric field at these junctions can split up the electrons and holes. Therefore, in addition to the MWCNTs acting as a pathway for the electrons collection, electrons and holes can travel toward their respective contacts, avoiding the recombination, and thus, the photo-to-current efficiency is enhanced. However, although in the mixture of $BiVO_4$ and MWCNTs, the MWCNTs were also participated in the electrons transfer, the heterojunction between $BiVO_4$ and MWCNTs is not formed and electric field does not exist, so the main photogenerated electrons were lost in the boundary between $BiVO_4$ and the MWCNTs. Therefore, the photocurrent was not enhanced greatly as expect.

4. Conclusions

The $BiVO_4$@MWCNTs nanocomposites were successfully fabricated by a soft-chemistry coprecipitation approach. An enhancement in the photocurrent over $BiVO_4$@MWCNTs composite electrode with respect to electrode of mixture of $BiVO_4$/MWCNTs as well as pure $BiVO_4$ was observed. It is concluded that the participation of MWCNTs acts as the electrons transfer media and the combination of $BiVO_4$ with MWCNTs tightly is beneficial for the electrons collection, resulting in that more electrons are able to transport quickly to the surface, which thus enhance the photo-to-current conversion efficiency.

Acknowledgments

This work was financial supported by the National Foundation of Natural Sciences (no. 20973097) and The National Basic Research Program of China (973 Program, 2009CB220000). The authors also thank Scientific Research Foundation for Returned Overseas Chinese Scholars for the financial support.

References

[1] A. Fujishima and K. Honda, "Electrochemical photolysis of water at a semiconductor electrode," *Nature*, vol. 238, no. 5358, pp. 37–38, 1972.

[2] A. Fujishima, T. N. Rao, and D. A. Tryk, "Titanium dioxide photocatalysis," *Journal of Photochemistry and Photobiology C*, vol. 1, no. 1, pp. 1–21, 2000.

[3] M. Grätzel, "Photoelectrochemical cells," *Nature*, vol. 414, no. 6861, pp. 338–344, 2001.

[4] M. R. Hoffmann, S. T. Martin, W. Choi, and D. W. Bahnemann, "Environmental applications of semiconductor photocatalysis," *Chemical Reviews*, vol. 95, no. 1, pp. 69–96, 1995.

[5] A. Millis and S. Le Hunte, "An review of semiconductor photocatalysis," *Journal of Photochemistry and Photobiology*, vol. 108, no. 1, pp. 1–35, 1997.

[6] H. Xu, C. Wu, H. Li et al., "Synthesis, characterization and photocatalytic activities of rare earth-loaded $BiVO_4$ catalysts," *Applied Surface Science*, vol. 256, no. 3, pp. 597–602, 2009.

[7] H. Xu, H. Li, C. Wu et al., "Preparation, characterization and photocatalytic properties of Cu-loaded $BiVO_4$," *Journal of Hazardous Materials*, vol. 153, no. 1-2, pp. 877–884, 2008.

[8] H. Xu, H. Li, C. Wu, J. Chu, Y. Yan, and H. Shu, "Nanoporous silicon explosive devices," *Materials Science and Engineering B*, vol. 147, article 52, 2008.

[9] M. Long, W. Cai, J. Cai, B. Zhou, X. Chai, and Y. Wu, "Efficient photocatalytic degradation of phenol over $Co3O_4$/$BiVO_4$ composite under visible light irradiation," *Journal of Physical Chemistry B*, vol. 110, no. 41, pp. 20211–20216, 2006.

[10] L. Ge, "Novel Pd/$BiVO_4$ composite photocatalysts for efficient degradation of methyl orange under visible light irradiation," *Materials Chemistry and Physics*, vol. 107, no. 2-3, pp. 465–470, 2008.

[11] Z.-G. Zhao and M. Miyauchi, "Nanoporous-walled tungsten oxide nanotubes as highly active visible-light-driven photocatalysts," *Angewandte Chemie—International Edition*, vol. 120, no. 37, pp. 7159–7163, 2008.

[12] J. Tang, Z. Zou, and J. Ye, "Photocatalytic decomposition of organic contaminants by Bi 2WO6 under visible light irradiation," *Catalysis Letters*, vol. 92, no. 1-2, pp. 53–56, 2004.

[13] T. Kako and J. Ye, "Photocatalytic decomposition of acetaldehyde over rubidium bismuth niobates under visible light irradiation," *Materials Transactions*, vol. 46, no. 12, pp. 2694–2698, 2005.

[14] H. Kato, H. Kobayashi, and A. Kudo, "Role of Ag^+ in the band structures and photocatalytic properties of $AgMO_3$ (M: Ta and Nb) with the perovskite structure," *Journal of Physical Chemistry B*, vol. 106, no. 48, pp. 12441–12447, 2002.

[15] H. G. Kim, D. W. Hwang, and J. S. Lee, "An undoped, single-phase oxide photocatalyst working under visible light," *Journal of the American Chemical Society*, vol. 126, no. 29, pp. 8912–8913, 2004.

[16] A. Kudo, "Development of photocatalyst materials for water splitting with the aim at photon energy conversion," *Nippon Seramikkusu Kyokai Gakujutsu Ronbunshi/Journal of the Ceramic Society of Japan*, vol. 109, no. 1270, pp. S81–S88, 2001.

[17] A. Kudo, "Development of photocatalyst materials for water splitting," *International Journal of Hydrogen Energy*, vol. 31, no. 2, pp. 197–202, 2006.

[18] Y. Hosogi, Y. Shimodaira, H. Kato, H. Kobayashi, and A. Kudo, "Role of Sn_{2+} in the band structure of SnM_2O_6 and $Sn_2M_2O_7$ (M = Nb and Ta) and their photocatalytic properties," *Chemistry of Materials*, vol. 20, no. 4, pp. 1299–1307, 2008.

[19] A. Kudo and I. Mikami, "New In_2O_3(ZnO)m pholocatalysts with laminai structure for visible light-induced H_2 or O_2 evolution from aqueous solutions containing sacrificial reagents," *Chemistry Letters*, no. 10, pp. 1027–1028, 1998.

[20] A. Kudo, K. Omori, and H. Kato, "A novel aqueous process for preparation of crystal form-controlled and highly crystalline $BiVO_4$ powder from layered vanadates at room temperature and its photocatalytic and photophysical properties," *Journal*

of the American Chemical Society, vol. 121, no. 49, pp. 11459–11467, 1999.

[21] S. Tokunaga, H. Kato, and A. Kudo, "Selective preparation of monoclinic and tetragonal $BiVO_4$ with scheelite structure and their photocatalytic properties," *Chemistry of Materials*, vol. 13, no. 12, pp. 4624–4628, 2001.

[22] A. Kudo, "Photocatalyst materials for water splitting," *Catalysis Surveys from Asia*, vol. 7, no. 1, pp. 31–38, 2003.

[23] J. Yu and A. Kudo, "Effects of structural variation on the photocatalytic performance of hydrothermally synthesized $BiVO_4$," *Advanced Functional Materials*, vol. 16, no. 16, pp. 2163–2169, 2006.

[24] K. Powell, "Getting schooled," *Nature*, vol. 435, no. 7043, pp. 850–851, 2005.

[25] K. Sayama, A. Nomura, Z. Zou, R. Abe, Y. Abe, and H. Arakawa, "Photoelectrochemical decomposition of water on nanocrystalline $BiVO_4$ film electrodes under visible light," *Chemical Communications*, vol. 9, no. 23, pp. 2908–2909, 2003.

[26] H. Luo, A. H. Mueller, T. M. McCleskey, A. K. Burrell, E. Bauer, and Q. X. Jia, "Structural and photoelectrochemical properties of $BiVO_4$ thin films," *Journal of Physical Chemistry C*, vol. 112, no. 15, pp. 6099–6102, 2008.

[27] H. Liu, R. Nakamura, and Y. Nakato, "Promoted photooxidation reactivity of particulate $BiVO_4$ photocatalyst prepared by a photoassisted sol-gel method," *Journal of the Electrochemical Society*, vol. 152, no. 11, pp. G856–G861, 2005.

[28] S. Iijima, "Helical microtubules of graphitic carbon," *Nature*, vol. 354, no. 6348, pp. 56–58, 1991.

[29] A. Kongkanand, R. M. Domínguez, and P. V. Kamat, "Single wall carbon nanotube scaffolds for photoelectrochemical solar cells. Capture and transport of photogenerated electrons," *Nano Letters*, vol. 7, no. 3, pp. 676–680, 2007.

[30] H. Ago, K. Petritsch, M. S. P. Shaffer, A. H. Windle, and R. H. Friend, "Composites of carbon nanotubes and conjugated polymers for photovoltaic devices," *Advanced Materials*, vol. 11, no. 15, pp. 1281–1285, 1999.